A Novel Role for α-Importins and Akirin in Establishment of Meiotic Sister Chromatid Cohesion in *Caenorhabditis elegans*

Richard Bowman, Nathan Balukoff, Talitha Ford, and Sarit Smolikove[1]
Department of Biology, University of Iowa, Iowa City, Iowa 52240
ORCID IDs: 0000-0002-3985-5482 (R.B.); 0000-0002-0146-2966 (T.F.); 0000-0003-0062-3606 (S.S.)

ABSTRACT During meiotic prophase I, sister chromatid cohesion is established in a way that supports the assembly of the synaptonemal complex (SC). The SC connects homologous chromosomes, directing meiotic recombination to create crossovers. In this paper, we identify two proteins that cooperate to import and load meiotic cohesins, thus indirectly promoting SC assembly. AKIR-1 is a protein with a previously identified meiotic role in SC disassembly. *akir-1* mutants have no obvious defects in sister chromatid cohesion. We identified *ima-2*, a gene encoding for an α-importin nuclear transport protein, as a gene interacting with *akir-1*. Analysis of *akir-1;ima-2* double mutants reveals a decrease in the number of germline nuclei and the formation of polycomplexes (PCs) (an SC protein aggregate). These PCs contain proteins that are part of the two main substructures of the SC: the central region and the lateral element. Unlike typical PCs, they also contain sister chromatid cohesion proteins. In *akir-1;ima-2* double mutants, PCs are located in both the nucleus and the cytoplasm. This suggests that the defects observed in the double mutants are both in nuclear import and in the assembly of sister chromatid cohesion. PC formation is also associated with recombination defects leading to reduced numbers of crossovers. Similarly to cohesion mutants, the pairing center protein HIM-8 is mislocalized in *akir-1;ima-2* double mutants, forming multiple foci. We propose that AKIR-1 and IMA-2 operate in parallel pathways to import and load chromosomally associated cohesin complex proteins in meiotic nuclei, a novel finding for both of these conserved proteins.

KEYWORDS AKIR-1; Akirin; COH-3/4; cohesin; cohesion; IMA-2; importin; meiosis; REC-8; synaptonemal complex

DURING meiotic prophase I, chromosome structure is modified such that it will support the formation of meiotically induced DNA double-strand breaks (DSBs) and their repair, to form crossovers and noncrossovers during recombination [reviewed in Zickler and Kleckner (1999)]. DSB formation and repair is essential for the proper segregation of homologous chromosomes during meiosis to form functional gametes, such as eggs and sperm. The process leading to the modification of meiotic chromosome structure initiates at the last DNA replication event prior to meiotic entry, during which sister chromatid cohesion complex proteins localize to the nucleus [reviewed in Mehta *et al.* (2013)

and Reichman *et al.* (2018)]. The meiotic sister chromatid cohesion complexes contain meiosis-specific cohesins as well as cohesins found in mitotic cells. They are typically composed of three subunits that are found in mitotic cohesion (Smc1, Smc3, and Scc3) and meiosis-specific Scc1-like protein(s) that replace the mitotic Scc1. In some organisms, other cohesion subunits are replaced as well. Cohesin loading is a regulated stepwise process that requires the cohesion loaders Scc2 and Scc4, and proteins involved in cohesion establishment such as Eco1 [reviewed in Litwin and Wysocki (2018) and Reichman *et al.* (2018)].

Proper assembly of the meiotic cohesion complex is required for the formation of the synaptonemal complex (SC) in a process termed synapsis (Zickler and Kleckner 1999; Reichman *et al.* 2018). The SC is a meiosis-specific protein complex that holds homologous chromosomes together, and is key for crossover formation and subsequent proper chromosome segregation during meiosis. The SC is divided into two substructures; the lateral elements, which form along

each chromosome, and the central element that connects the two lateral elements of homologs to form the SC. When lateral elements are not yet assembled they are referred to as chromosomal axes. The SC is imperative to meiosis, as one important role for the SC is to increase the efficiency of homology searching that takes place during meiotic recombination, leading to the repair of meiotic DSBs as crossovers.

In *Caenorhabditis elegans*, three meiotic sister chromatid cohesion complexes can be formed containing SCC-1-like proteins: REC-8 or COH-3, and COH-4 (Pasierbek *et al.* 2001; Severson *et al.* 2009; Severson and Meyer 2014). COH-3 and COH-4 are nearly identical and thus are frequently referred together; COH-3/4 (Severson and Meyer 2014). These cohesins cooperate in the recruitment of HTP-3, a lateral element component of the SC that is also essential for DSB formation (Goodyer *et al.* 2008). HTP-3 is required for the assembly of REC-8, but not COH-3/4, on meiotic chromosomes. HTP-3 also recruits HIM-3 and HTP-1/2, proteins that are part of the lateral elements (Couteau and Zetka 2005; Martinez-Perez and Villeneuve 2005). The central region of the SC is composed of a family of proteins that are interdependent in their localization; SYP-1/2/3/4 (MacQueen *et al.* 2002; Colaiácovo *et al.* 2003; Severson 2009). The localization of the SYP proteins (SYPs) is completely dependent on lateral element proteins, but the SYPs are dispensable for the localization of cohesin or lateral element proteins.

The roles that sister chromatid cohesion and SC assembly play in meiosis, and the meiotic mechanisms involving these proteins, are evolutionarily conserved. However, in *C. elegans* the initial association of chromosomes prior to complete synapsis involves a unique mechanism: the recruitment of pairing center proteins to pairing centers, which are found at one end of each chromosome (MacQueen *et al.* 2005; Phillips and Dernburg 2006). The pairing center proteins colocalize with Sad1 and UNC-84(SUN)/Klarsicht, ANC-1, Syne homology (KASH) domain proteins [the Linker of Nucleoskeleton and Cytoskeleton (LINC) complex], which span the nuclear envelope and connect the chromosomes to the cytoskeleton (Penkner *et al.* 2007; Sato *et al.* 2009). The movement of chromosomes via cytoskeleton-associated motor proteins is conserved and essential for synapsis in *C. elegans*, as in many other organisms (Alleva and Smolikove 2017).

The assembly and disassembly of the SC is a tightly regulated process. In some mutants, SC proteins aggregate and form dysfunctional SC structures termed polycomplexes (PCs). SC misassembly that is manifested in PCs leads to defects in recombination, frequently leading to a reduction in the number of crossovers [for example, Smolikov *et al.* (2008) and Alleva *et al.* (2017)]. PCs are frequently found at the time of SC assembly, but they are rarely observed at the time of SC disassembly (Clemons *et al.* 2013). In *C. elegans*, Akirin/AKIR-1 loss-of-function leads to PC formation upon SC disassembly, although SC assembly proceeds normally in these mutants (Clemons *et al.* 2013). While the exact function of AKIR-1 in *C. elegans* meiosis is unknown, studies of the

innate immune response in *C. elegans* identified AKIR-1 as interacting with the nucleosome remodeling and deacetylase (NuRD) chromatin remodeling complex (Polanowska *et al.* 2018). This function is similar to what is observed in other organisms, where Akirin affects transcription through its interaction with transcription factors and/or the SWItch/sucrose non-fermentable (SWI/SNF) chromatin remodeling complex (Komiya *et al.* 2008; Nowak *et al.* 2012; Tartey *et al.* 2014, 2015; Liu *et al.* 2017). Akirin lacks a DNA-binding domain and thus was suggested to serve as a protein connecting transcription factors to chromatin remodelers (Nowak *et al.* 2012). Akirin's function in the germline has not been reported except in *C. elegans* (Clemons *et al.* 2013). Akirin has diverse somatic functions that include a role in tumor promotion and the immune response (de la Fuente *et al.* 2006; Goto *et al.* 2008; Komiya *et al.* 2008), and in the development of muscles and the nervous system (Marshall *et al.* 2008; Nowak *et al.* 2012; Chen *et al.* 2015; Bosch *et al.* 2016; Liu *et al.* 2017). The lack of studies of the meiotic function for Akirin makes it difficult to speculate the exact molecular function of Akirin in meiosis.

The function of the germline requires, as do other tissues, regulated import of proteins into the nucleus (Goldfarb *et al.* 2004; Adam 2009). Nuclear import is a conserved process in which proteins transported into the nucleus pass through the nuclear pore complex bound by proteins from the conserved family of importins. This allows the nuclear entry of large proteins and protein complexes. The importins are divided into two subfamilies: α- and β-importins (IMA and IMB, respectively). One member from each family forms a dimer that binds a cargo protein and, in turn, associates with the nuclear pore complex for transit from the cytoplasm into the nucleus. Surprisingly α-importins were implicated in the regulation of transcription directly, outside of their role in nuclear import [reviewed at Miyamoto *et al.* (2016)]. In *C. elegans*, there are three IMA proteins (IMA-1, IMA-2, and IMA-3) and three IMB proteins (IMB-1, IMB-2 and IMB-3) (Adam 2009). All three IMA proteins are germline expressed, but while IMA-2 and IMA-3 are expressed throughout the germline, the expression of IMA-1 is restricted to late meiotic prophase I (Geles and Adam 2001). RNA interference (RNAi) studies indicate that *ima-2* is required for regulating germline size, but the mechanism by which IMA-2 acts as well as its germline cargo(s) are unknown (Geles *et al.* 2002).

Here, we explore additional germline functions of AKIR-1 and IMA-2 in *C. elegans*. We report evidence of a role for these proteins in loading of meiotic cohesins, thus supporting the formation of the SC. This redundancy between AKIR-1 and the α-importin IMA-2 prevented the previous discovery of these functions by the analysis of single mutants. In the absence of IMA-2 and AKIR-1, PCs are formed and aberrantly recruit cohesins into this structure. These PCs impede recombination and crossover formation. The lack of sister chromatid cohesion also impairs the localization of a pairing center protein. Our studies indicate a novel role for Akirin and point to cohesins as possible targets for IMA-2 in nuclear import in the germline.

Materials and Methods

Strains

All strains were cultured at 20° on NGM plates spread with OP50 bacteria. Bristol N2 strain was used as a wild-type control. Strains used were *akir-1(gk528)*I, *ima-1(tm7139)*V, *ima-2(ok256)*I, *ima-3(ok715)*IV, *csn-5(ok1064)*IV, *akir-1(gk528)*I;*ima-1(tm7139)*V, *akir-1(gk528)*I;*ima-2(ok256)*I, *akir-1(gk528)*I;*ima-3(ok715)*IV, and *rec-8(ok978)*IV;*coh-3(gk112)*V;*coh-4(tm1857)*V. Transgenic lines used were *3xflag::akir-1*(I), *ojIs9 [zyg-12(all)*II::*GFP + unc-119(+)*III*]*, *akir-1(iow37[3xflag::akir-1])*, *akir-1(iow86[3xflag::akir-1])*(I);*ima-2(ok256)*I, *hT2 [qls48; akir-1(iow32[FLAG::akir-1]] (I,III)*, *akir-1(gk528)*I; *ojIs9 [zyg-12(all)*II::*GFP + unc-119(+)*III*]*, *ima-2(ok256)*I; *ojIs9 [zyg-12(all)*II::*GFP + unc-119(+)*III*]*, and *akir-1(gk528)*I;*ima-2(ok256)*I; *ojIs9 [zyg-12(all)*II::*GFP + unc-119(+)*III*]*.

Clustered regularly interspaced short palindromic repeat/Cas9 genome modification

The desired area for the insertion in the target gene was identified and Protospacer Adjacent Motif (PAM) sites for the desired area were identified. One sequence was selected (5′-GATTCATACTCGTGTTGCAG-3′), for which crRNA was ordered. For *3xflag* insertion (Paix *et al.* 2014), an single-stranded oligodeoxynucleotide (ssODN) was designed containing the *3xflag* sequence preceded by the AUG start codon and flanked by homology arms that contain four silent mutations (sequence: 5′-TTACTTCTCGTAACCACAAATTATTT CTTTCAGAAGTAAAATGgactacaaagaccatgacggtgattataaa gatcatgatatcgattacaaggatgacgatgacaagGCTTGCGGACTCG CACTGAAAAGACCTCTCCAACATGAGTACGAGTCTTTTTT AACTGATGAGACATACAACGGAGAAGCAAAGCGAGCC-3′). The microinjection protocol was followed as in Paix *et al.* (2016). In short, Bristol N2 larval stage 4 (L4) were selected and placed onto agar plates spread with OP50 bacteria. They were incubated overnight at 20°, and the next day hermaphrodite gonads were microinjected with a mix of the crRNA, co-injection marker (*dpy-10*), and ssODN. Injected worms were placed singly onto OP50 spread agar plates and their offspring were monitored for the presence of the co-injection marker. These worms were subjected to PCR assay flanking the insertion site and insertion was confirmed by Sanger sequencing as *akir-1(iow37[3xflag::akir-1])*. Since *akir-1* and *ima-2* are linked, a similar protocol was followed for injection of *ima-2(ok256)/hT2* to generate *akir-1(iow86[flag::akir-1]; ima-2(ok256) I/hT2 [qls48; akir-1(iow32[flag::akir-1]] (I,III)*, except that injections were done in two steps: one to integrate the *3xflag* into the balancer chromosome and the second to integrate *3xflag* into the chromosome containing *ima-2(ok256)*. *akir-1(iow37[3xflag::akir-1])*(I) was outcrossed twice.

Dissection

Each genotype was selected at L4 and placed onto agar plates spread with OP50 bacteria. They were incubated for 21–24 hr at 20°. Day 1 hermaphrodites were placed 15 at a time in 15 μl drops of M9 buffer. These adults were midbody dissected to release the gonads using a razorblade.

Immunostaining and microscopy

Worms from each genotype were collected at L4 and incubated for 21–24 hr at 20°. After incubation, 15 adult hermaphrodites were placed in 15 μl M9 buffer on a slide coverslip and dissected at the center of the body to release the gonads. After dissection, the slides were flash frozen on dry ice and dipped in −20° methanol for 1 min. They were then fixed with 4% paraformaldehyde (PFA) for 30 min, blocked with 0.5% BSA for 1 hr, and incubated with the appropriate primary antibody in PBS Tween (PBST) at room temperature overnight. The slides were then rinsed in PBST and incubated in the appropriate secondary antibody at room temperature for 2 hr, rinsed and stained with DAPI in PBST, and mounted with Vectashield. Primary antibodies used were: rabbit anti-RAD-51 (1:10,000; Model Organism ENCyclopedia Of DNA Elements), goat anti-SYP-1 (1:500), rabbit anti-SYP-2 (1:500), rabbit anti-COH-3/4 (1:500, gift from A. Severson), guinea pig anti-HTP-3 (1:500, gift from M. Zetka), rabbit anti-SUN-1 (1:500; SDIX), rabbit anti-REC-8 (1:1000; SDIX), rabbit anti-HIM-8 (1:1000; SDIX), mouse IgG1 anti-FLAG (1:100; Sigma [Sigma Chemical], St. Louis, MO), and rabbit anti-SMC-3 (1:1000; Novus). Secondary antibodies used were: bovine anti-goat (1:500), donkey anti-goat (1:500), donkey anti-rabbit (1:500), goat anti-rabbit (1:500), donkey anti-mouse IgG (1:500), and goat anti-guinea pig (1:500). All images, except Figure 1D and E, are projections through three-dimensional (3D) stacks of whole nuclei and were taken with a DeltaVision wide-field fluorescence microscope (Applied Precision) with an Olympus 100×/1.40-numerical aperture lens. Optical sections are at 0.20 μm increments taken with the coolSNAPHQ camera (Photometrics) and viewed with softWoRx software (Applied Precision). The images were deconvolved using SoftWoRx 5.0.0 software (Applied Precision).

Intensity measurement

Intensity was calculated in FIJI/ImageJ using the following formula: Nuc(RawIntDen/Area) − background(RawIntDen/Area). Slides for all three genotypes examined were processed together and images acquired under the same exposure conditions (*n* images for "zones" 1, 3, and 5, and diakinesis-2 and -1: wild-type = 4, 5, 5, and 8, *3xflag::akir-1* = 7, 6, 9, and 19, and *3xflag::akir-1*; *ima-2* = 7, 6, 7, and 32). Nondeconvolved, midsection slice, raw image files were used for quantification. For each image taken from zones, five nuclei were randomly selected and traced based on the DAPI channel of each nucleus. Diakinesis images contain one nucleus, which was selected for analysis. Background was taken from two regions outside nuclei, but inside the germline (nuclei identified based on DAPI). Once a region was identified on the DAPI channel, images were switched to the anti-FLAG antibody channel for quantification of the selected region.

Nuclei and oocyte number quantification

The number of nuclei in each gonad for each genotype was determined by taking a one-half thickness image of the nuclei in 512 × 512 pixel images along the length of the gonad from the premeiotic tip (PMT) through late pachytene. The number of nuclei was counted in a half-Z-stack 3D image. The number of diakinesis nuclei in each gonad for each genotype was determined by counting the number of single-row nuclei postdiplotene through the final oocyte prior to the spermatheca.

Meiotic phase designation and SC quantification

The stages of meiosis were determined by the location of each nucleus and its chromosomal morphology (via DAPI) combined with staining for SYP proteins. The mitotic nuclei (also called premeiotic nuclei) are found before chromosome polarization initiates and are characterized by the lack of SYP localization to DNA. Early prophase nuclei are those entering prophase from the premeiotic region, and are characterized by partially polarized chromosomal organization and a partial accumulation of SYP proteins on DNA. Middle prophase nuclei are found approximately midway between the distal tip and the bend of the gonad, and are characterized by visibly linear chromosomes and SYP proteins localized along the length of the DNA. This methodology was also used to identify the appearance of aberrant cohesin and SC localization patterns. The cohesin REC-8 and the cohesin subunit SMC-3 begin to accumulate on the DNA during mitosis in wild-type worms, and are fully associated along the length of the DNA at entry into prophase. The cohesins COH-3/4 and the SC components HTP-3, SYP-1, and SYP-2 follow the pattern outlined in the previous paragraph. The wild-type *C. elegans* gonad from the PMT through late pachytene is seven zones long, with a single zone encompassing a 512 × 512 (32.91 μm) pixel region using the 100× objective.

RAD-51 focus quantification

Quantification of RAD-51 foci numbers was performed in each "zone" of the *C. elegans* gonad by counting the number of foci in a 3D stack.

DAPI body quantification

The number of DAPI bodies was counted in 3D images taken from diakinesis-1 oocytes.

HIM-8 quantification

The number of HIM-8 foci per nucleus was counted in each zone. The wild-type number of foci was two per nuclei during mitotic proliferation and one focus after entry into meiotic prophase I (indicating that the X-chromosomes have paired). Any number higher than two was scored as "many." The location of the foci was characterized as inside the nucleus, associated with the nucleus, or cytoplasmic, and was determined by whether a particular focus contacted the nuclear membrane SUN/KASH protein ZYG-12 or not.

SUN-1 quantification

SUN-1 localization pattern was quantified as either patchy or dispersed in each zone by discontinuous or continuous localization, respectively, at the midnucleus slice of the 3D stack.

Movement quantification

Imaging was measured as in Alleva *et al.* (2017). In short, 2–3-min recordings at 60 frames per minute were taken of GFP-tagged ZYG-12 in the genotypes examined. To quantify the movement of ZYG-12 foci, each nucleus was examined to find a ZYG-12 focus that stayed in focus for 60 consecutive seconds. Each change in direction was recorded, as was the period of time that there was no movement. The distance traveled was calculated as the sum of the distance traveled in 1 min, and velocity was calculated by dividing the distance traveled by 60 sec.

Statistical analysis

Any data that had discrete numerical values were tested for significance with the Mann–Whitney *U*-test (MW test) using GraphPad Prism 7 software.

Data availability

Strains are available upon request. The authors state that all data necessary for confirming the conclusions presented in the article are represented fully within the article. Supplemental material available at Figshare: https://doi.org/10.25386/genetics.7471409.

Results

Loss of both AKIR-1 and IMA-2 results in reduced gonad size, and aberrant diakinesis oocyte formation

To identify the mechanisms by which AKIR-1 acts in meiosis we sought out the proteins that physically interact with AKIR-1 using the yeast two-hybrid system. We performed the screen for AKIR-1 interactions to saturation (1.6×10^6 colonies) and identified 111 interactions with sequences encoding for *C. elegans* proteins. From these 111 sequences, 92 sequences aligned to IMA-2 cDNA. Next, we investigated the genetic interaction between IMA-2 and AKIR-1. *akir-1(gk528)* deletion mutants show defects in SC disassembly without any visible effects on SC assembly (Clemons *et al.* 2013). Knockdown of *ima-2* by RNAi was previously described as having an effect on gonad size (Geles *et al.* 2002), but no other meiotic aspects of *ima-2* depletion were investigated. We employed mutants of *akir-1* and *ima-2*, which are expected to be null, to determine their meiotic function.

Qualitative analysis of gonad morphology in the *akir-1(gk528)* and *ima-2(ok256)* single mutants, as well as the double mutant *akir-1(gk528);ima-2(ok256)*, indicated that the overall gonad length was shorter than wild-type in all of these three genetic backgrounds (Supplemental Material, Figure S1). To quantify the reduced gonadal size and identify
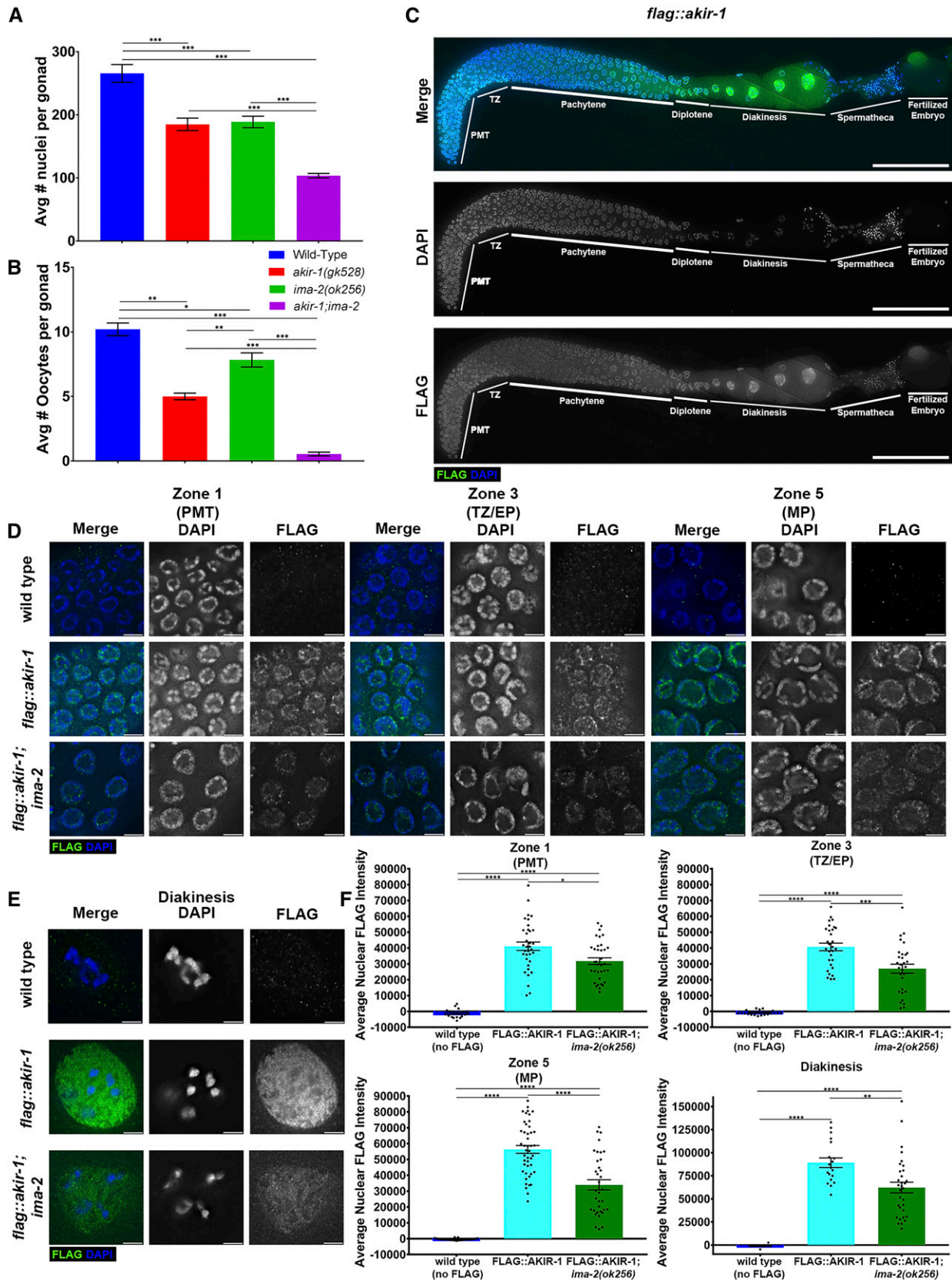
Figure 1 Loss of AKIR-1 and IMA-2 results in reduced gonad size, and aberrant diakinesis oocyte formation; AKIR-1 localizes to germline nuclei. (A) The average number of nuclei present in the germline for each genotype from the PMT through late pachytene for each indicated genotype was measured by taking a three-dimensional image from the center of the syncytium to the outer nuclei, counting each nuclei in the stack, and doubling the number

the population of nuclei affected, we performed DAPI staining of 1 day post-L4 adult hermaphrodites of wild-type and all three mutant strains, and examined their germlines. Nuclei are arranged in the germline in a way that their position reflects their meiotic stage. Nuclei at the distal germline are proliferating mitotically, a region termed the PMT, and enter meiosis in the transition zone (TZ), the leptotene–zygotene meiotic prophase I stage. Nuclei then progress to the pachytene stage which is subdivided to early, middle, and late pachytene regions (EP, MP, and LP, respectively). The proximal gonad contains diakinesis nuclei, which are the last stage of meiotic prophase I. To analyze germline size, we counted nuclei from the PMT through LP (Figure 1A, n values for all figures are presented in Table S1) as well as the number of diakinesis oocytes (Figure 1B). The number of nuclei in both akir-1(gk528) and ima-2(ok256) gonads was reduced, as compared to wild-type (number for one-half a germline 265.7 vs. 184.9 and 188.8, respectively, $P < 0.0001$, MW test), but similar to each other ($P = 0.7606$, MW test). The number of nuclei in akir-1(gk528);ima-2(ok256) was even further reduced as compared to each single mutant, showing an additive effect (103.6, $P < 0.0001$ for all pairwise comparisons, MW test). A similar effect was observed when counting the number of diakinesis nuclei; we found a reduction in the number of diakinesis oocytes in akir-1(gk528) mutants as compared to wild-type (5 vs. 10.2, $P = 0.0043$, MW test, Figure 1B), as well as in ima-2(ok258) mutants as compared to wild-type (7.83 vs. 10.2, $n = 6$ and 5 gonads, respectively, $P = 0.0195$, MW test). The number of oocytes was further reduced in the akir-1(gk528);ima-2(ok256) double mutants as compared to wild-type (0.54 vs. 10.2, $P = 0.0001$, MW test) or single mutants ($P = 0.0043$, $P < 0.0001$, MW test). Next, we counted the number of eggs laid and their hatching rate. akir-1(gk528) mutants show reduction in both the numbers of eggs laid (117 ± 38 eggs/worm compared to 269 ±/−21 eggs/worm in wild-type) and their hatching rate (38% compared to 100% in wild-type n eggs = 808 and 654), as previously published (Clemons et al. 2013). ima-2(ok258) mutants laid eggs in comparable numbers to wild-type (214 ± 48 eggs/worm), but these eggs did not hatch (0% $n = 664$ eggs). No males were observed among the hatched progeny of all genotypes. Five akir-1(gk528);-ima-2(ok256) double mutants for 4 days post-L4 laid no eggs, indicating that the double mutant is completely sterile. These data show an additive phenotypic effect between akir-1(gk528)

and ima-2(ok256) alleles, suggesting that AKIR-1 and IMA-2 are both required for gonad development.

AKIR-1 localizes to germline nuclei, which is partially dependent on IMA-2

IMA-2 was shown to localize to germline cytoplasm and was enriched in nuclei throughout the germline (Geles and Adam 2001). AKIR-1 was found to be a germline-expressed protein but its precise localization in the germline was unknown (Polanowska et al. 2018). To identify the localization pattern of AKIR-1 in the germline, we inserted a FLAG tag at the N-terminus of AKIR-1, after the AUG using clustered regularly interspaced short palindromic repeat/Cas9 (Paix et al. 2014, 2016). akir-1 null mutants were shown to have a reduced brood size (Clemons et al. 2013). However, the flag::akir-1 strain is viable and fertile, indicating that the tag does not interfere with AKIR-1 function.

akir-1 null mutants show defects in SC disassembly starting in late pachytene, with no obvious defects in mitosis or early meiotic prophase I (Clemons et al. 2013). Consistent with these findings, AKIR-1 is expressed in late pachytene and in all diakinesis nuclei. However, AKIR-1 is also expressed in the other germline regions and localizes adjacent to DAPI (Figure 1, C–E). Quantitative analysis of anti-FLAG staining indicates that AKIR-1 is enriched in nuclei throughout the germlines, but is twice as abundant in diakinesis nuclei (Figure 1F). These data indicate that AKIR-1 is found in nuclei prior to where a phenotype is seen in the akir-1 single mutant. The PMT localization of AKIR-1 is likely to reflect an additional role for AKIR-1 that is redundant with another protein(s). The additive effect observed in akir-1(gk528);ima-2(ok256) double mutants suggests that these redundant functions are between AKIR-1 and IMA-2.

The physical interaction between AKIR-1 and IMA-2 (yeast two-hybrid) suggest that these two proteins act in the same pathway. However, the redundancy found in genetic interactions indicates that AKIR-1 and IMA-2 are part of two distinct pathways. We therefore examined if AKIR-1 localizes to germline nuclei in the absence of IMA-2. Indeed, AKIR-1 localization to germline nuclei was found in ima-2(ok256) mutants, but at reduced levels (Figure 1, D–F). These data indicate that AKIR-1's localization to germline nuclei is partially dependent on IMA-2. However, AKIR-1 can localize to germline nuclei in the absence of IMA-2, consistent with a partially redundant function.

($n = 3$ gonads), with significance between genotypes indicated by the asterisks. (B) The average number of oocytes in a single row from the bend through diakinesis-1 ($n = 3$ gonads), with significance between genotypes indicated by the asterisks ($P < 0.05$, Mann–Whitney U-test). (C) AKIR-1 localization in 3XFLAG::AKIR-1 germline nuclei during mitotic proliferation, and early and middle prophase. Blue is DAPI and green is AKIR-1 (anti-FLAG). Bar, 50 μm. (D and E) AKIR-1 localization in wild-type (negative staining control), 3xflag::akir-1, and 3xflag::akir-1 ima- 2(ok256) in the germline indicated regions, single stack from midsection, deconvolved. Blue is DAPI and green is AKIR-1 (anti-FLAG). Bar, 3 μm. (F) Quantification of intensity of nuclear staining of FLAG::AKIR-1 in wild-type and ima-2 mutants normalized to cytoplasmic staining with significance between genotypes indicated by the asterisks. For n values for (A and B) see Table S1, for (F) n nuclei are indicated by the data points on the graph. $P < 0.05$, * $0.05 < P > 0.01$, ** $0.01 < P > 0.001$, *** $0.001 < P > 0.0001$, and **** $0.0001 < P$; Mann–Whitney U-test. Avg, average; EP, early pachytene; MP, midpachytene; PMT, premeiotic tip; TZ, transition zone.
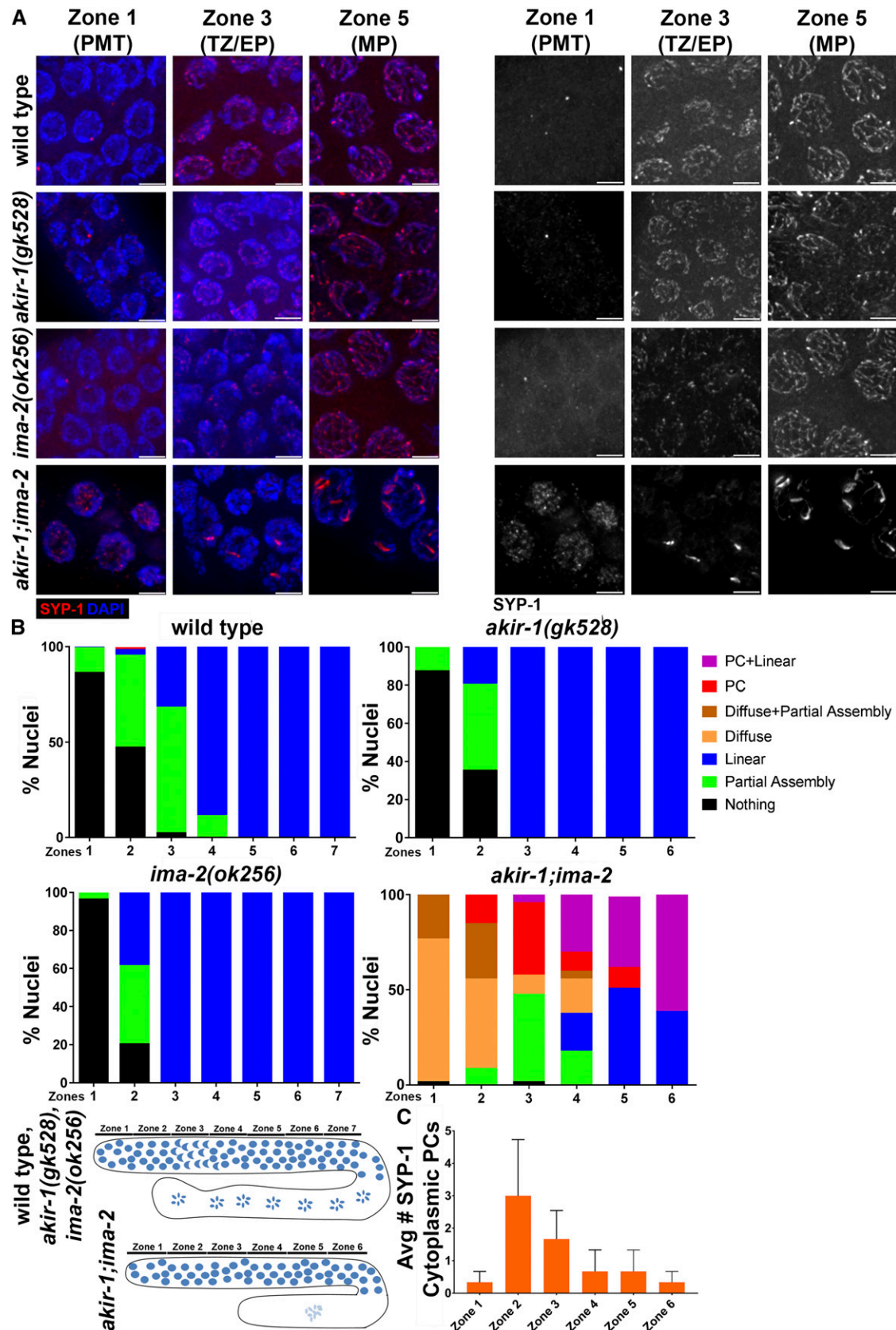
Figure 2 The loss of AKIR-1 and IMA-2 causes SYP PC formation. (A) Immunolocalization of SC central region protein SYP-1 for the genotypes indicated. Antibody only channel is presented on the right. In *akir-1(gk528);ima-2(ok256)* germline SYP-1 is mislocalized. Bar, 3 μm. (B) Quantification of SYP-1 localization phenotypes showing aberrant central region appearance in the double mutant *akir-1 ;ima-2*. Localization was classified as follows:

The loss of both AKIR-1 and IMA-2 causes PC formation

akir-1(gk528) mutants show defects in the disassembly of the SC that are specific to the central region of the SC (Clemons *et al.* 2013). The SC is composed of two main substructures: the central region and the lateral elements (referred to as axis proteins, in their nonassembled form). To determine the role of AKIR-1 and IMA-2 on the assembly or disassembly of the SC, we examined the localization of SYP-1 (a central region protein) and HTP-3 (a lateral element/axis protein). In the wild-type germline, SYP-1 partially assembled in the TZ and localized along the entire length of the homologs in pachytene. We found no difference in the localization pattern of SYP-1 from meiotic entry, at the TZ, through pachytene in *akir-1(gk528)* mutants [as previously reported (Clemons *et al.* 2013)], or *ima-2(ok256)* mutants compared to wild-type (Figure 2, A and B). However, in *akir-1(gk528);ima-2(ok256)* double mutants, we observed an aberrant localization of SYP-1 in all regions of the gonad (Figure 2, A and B). Moreover, in the wild-type PMT, SYP-1 was either not present or was found in puncta, while in *akir-1(gk538);ima-2(ok256)* double mutants SYP-1 was diffuse in the PMT nuclei. In wild-type worms and the two single mutants, meiotic entry is accompanied by chromosome clustering in the TZ, when they localize to one side of the nuclear periphery. In *akir-1(gk538);ima-2(ok256)* double mutants, clustered chromosomal morphology was found intermingled with nuclei with pachytene-like morphology (dispersed chromosomes) throughout the germline, lacking a defined TZ. In *akir-1(gk538);ima-2(ok256)* double mutants, instead of SYP-1 forming a linear pattern along chromosomes (as seen in pachytene in wild-type and the single mutants), SYP-1 only partially assembled and formed large PCs, starting in EP nuclei (Figure 2, A and B). Cytoplasmic PCs were never found in wild-type or single mutants, but in *akir-1(gk538);ima-2(ok256)* double mutants PCs were found in the cytoplasm, mainly in early meiotic prophase I (Figure 2C and Figure S9). As nuclei progressed through pachytene (zones 5 and 6), nuclei containing PCs also exhibited some linear assembly along the chromosomes (Figure 2B, purple). Similar localization patterns were found for SYP-2, another central region protein.

To examine if the effects on SC assembly were specific to AKIR-1's interaction with IMA-2, we examined SYP-1 localization for the other two α-importins *ima-1(tm7139)* and *ima-3(ok715)*, as well as *ima-1(tm7139);akir-1(gk528)* and *ima-3(ok715);akir-1(gk528)* double mutants. No defects in SYP-1 localization were observed in any one of these mutants, indicating that the defects in SC assembly are specific to AKIR-1's interaction with IMA-2 and not interaction with any α-importin (Figure S2).

PCs can be composed only of central region proteins [*e.g.*, *csn-5* mutants (Brockway *et al.* 2014)] or of all SC proteins [*e.g.*, *htp-3(RNAi)* (Goodyer *et al.* 2008)]. To test if defects in SC assembly in *akir-1(gk528);ima-2(ok256)* double mutants are specific to central region proteins, we examined lateral/axial element HTP-3 localization. *akir-1(gk528)* or *ima-2(ok256)* single mutants showed no defects in lateral element assembly (Figure 3, A and B; Clemons *et al.* 2013). However, in the double mutant *akir-1(gk528);ima-2(ok256)* we found partial assembly of HTP-3 along chromosomes as well as PCs. Similar to our previous observation with SYP-1, HTP-3 PCs were found in nuclei (Figure 3, A and B) as well as in the cytoplasm (Figure 3C).

Because HTP-3 and SYP-1/SYP-2 form PCs in *akir-1(gk528);ima-2(ok256)* double mutants, we tested whether central region and lateral element PCs were part of the same PC structure. We examined the colocalization between the two proteins by immunostaining for both SYP-2 and HTP-3. We found that SYP-2 and HTP-3 colocalized in meiotic nuclei of all genotypes, including in the PCs formed in the *akir-1(gk528);ima-2(ok256)* double mutants (Figure S3). Since central region assembly is dependent on lateral/axial elements (*e.g.*, Smolikov *et al.* 2007), these data suggest that the loss of AKIR-1 and IMA-2 affects the efficient loading of axis proteins, which in turn affects the loading of SC central region proteins.

Loss of both AKIR-1 and IMA-2 results in defects in meiotic recombination

The assembly of the SC is important for efficient meiotic recombination, therefore we expected that the repair of meiotic DSBs would be delayed by the loss of both AKIR-1 and IMA-2. RAD-51 is a marker of recombination intermediates due to its localization to single-stranded DNA (ssDNA) formed by the processing of SPO-11-induced DSBs; in the absence of SC, RAD-51 is loaded on ssDNA at the sites of DSBs but it accumulates on chromosomes at higher levels than observed in wild-type (Colaiácovo *et al.* 2003). Despite their apparent lack of defects in SC assembly, single mutants of *akir-1(gk528)* or *ima-2(ok256)* showed a small decrease in the average number of RAD-51 foci [Figure 4, A and B (Clemons *et al.* 2013)]. Since lateral element assembly is required for DSB formation, this may indicate that axis assembly in these mutants is mildly impaired, but not to the level seen in immunolocalization studies. Consistent with the defects in SC assembly in *akir-1(gk528);ima-2(ok256)* double mutants, they also displayed a significant increase in RAD-51 foci numbers in most gonadal zones (Figure 4B). However, the increases in RAD-51 foci numbers in *akir-1(gk528);ima-2(ok256)* double mutants were not as large as observed in

no staining (black), partially assembled SYP-1 (green), SYP-1 assembled SC (blue), nuclear localization in form of a haze with no specific pattern (tan), nuclei with partially assembled SYP-1 as well as nonspecific diffuse localization (brown), nuclei with PC (red), or linear and PC in the same nucleus (purple), and wild-type-appearing nuclei with SYP-1 fully linear along homologous chromosomes. A cartoon representing division by zones is indicated on the bottom. (C) Quantification of cytoplasmic SYP-1 PCs throughout the germline of the double mutant *akir-l;ima-2* (*n* = 3 gonads). For *n* values see Table S1. Avg, average; EP, early pachytene; MP, midpachytene; PC, polycomplex; PMT, premeiotic tip; SC, synaptonemal complex; TZ, transition zone.
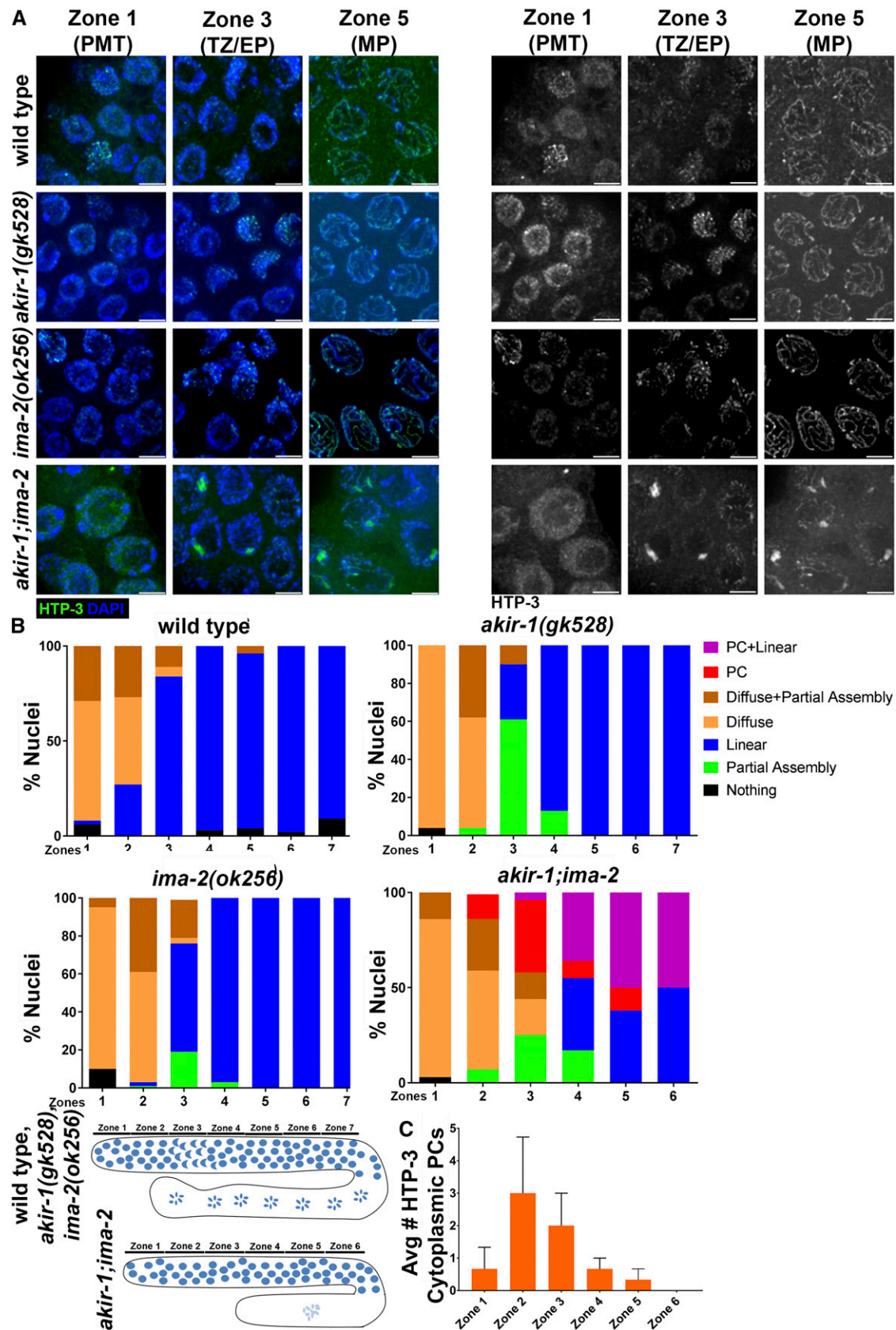
Figure 3 The loss of AKIR-1 and IMA-2 causes HTP-3 PC formation. (A) Immunolocalization of the SC lateral element protein HTP-3 for the genotypes indicated. Antibody only channel is presented on the right. Bar, 3 μm. (B) HTP-3 is mislocalized in *akir-l(gk528);ima-2(ok256)* double mutants. Key is
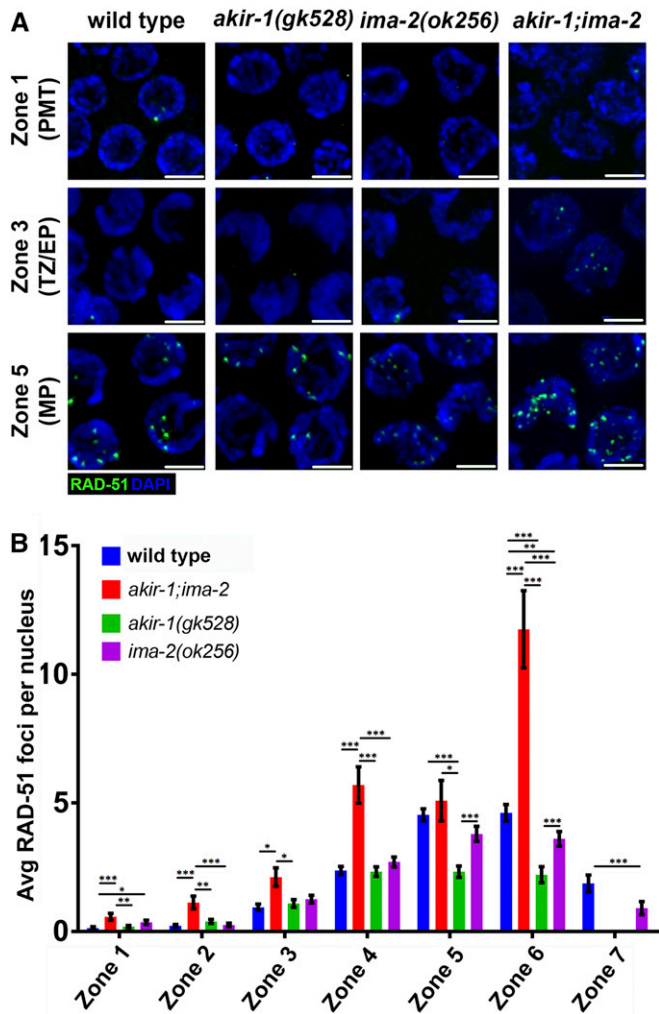
Figure 4 Loss of AKIR-1 and IMA-2 results in defects in the repair of meiotic DSBs. (A) Immunolocalization of RAD-51 for the genotypes indicated. Wild-type worms, and both single mutants *akir-l(gk528)* and *ima-2(ok256)*, are visually indistinguishable from each other; *akir- l-(gk528);ima-2(ok256)* has a visually distinct increase in the number of RAD-51 foci in middle prophase. Bar, 3 μm. (B) Quantification of the average number of RAD-51 foci per nucleus in the gonad from the premeiotic tip through late pachytene for all genotypes including the average number of RAD-51 foci found in *csn-5(okl064)* mutants (Brockway *et al.* 2014). Significance between genotypes indicated by asterisks ($P \leq 0.05$, * $0.05 \leq P \geq 0.01$, ** $0.01 < P \geq 0.001$, and *** $0.001 < P \geq 0.0001$); Mann–Whitney *U*-test). For *n* values see Table S1. Avg, average; DSB, double-strand break; EP, early pachytene; MP, midpachytene; PMT, premeiotic tip; TZ, transition zone.

csn-5(ok1064) mutants, which only impairs the assembly of central region proteins (Brockway *et al.* 2014).

Repair of meiotic DSBs leads to the formation of crossovers, manifested as bivalents that are easily observed in the first diakinesis oocyte prior to fertilization (diakinesis-1). Each of the single mutants and wild-type displayed six DAPI staining

bodies ($n = 10$ gonads) at diakinesis-1, indicating that crossovers had formed. When analyzing *akir-1(gk528);ima-2 (ok256)* gonads, we observed that only 31% of diakinesis-1 oocytes had six bivalents (Figure 5, A and B). In 38% of diakinesis-1 nuclei analyzed, more than six univalents were present, one-half of which had 11–12 univalents, indicating an inability to form crossovers. The remaining 31% of double mutant diakinesis-1 nuclei exhibited clumped DAPI masses suggestive of repair by a mechanism that does not rely on homologous recombination. Interestingly, all three phenotypes could be found in the same worm, and even within the same gonad (Figure 5C). Taken together, these results suggest that the loss of both AKIR-1 and IMA-2 results in defects in meiotic DSB repair; however, these are only found in about one-half of the oocytes.

Impaired SC assembly in akir-1(gk528);ima-2(ok256) double mutants is not due to defects in ZYG-12 patch formation or movement

In *C. elegans*, chromosomal pairing centers are tethered to the nuclear envelope by the LINC complex (SUN-1/ZYG-12) to promote chromosome movement (Penkner *et al.* 2007). This movement is essential for proper synapsis. Therefore, we examined if ZYG-12 patch formation and its movement was affected in *akir-1(gk528);ima-2(ok256)* double mutants. We found no difference in SUN-1 localization between wild-type and any one of the three mutant genotypes examined [*akir-1(gk528)*, *ima-2(ok256)*, and *akir-1(gk528);ima-2(ok256)* double mutants] in early prophase (Figure S4). Moreover, LINC movement (monitored by live imaging of ZYG-12) did not decrease in *akir-1(gk528);ima-2(ok256)* mutants (Figure S5). Taken together, these data suggest that the defects in SC assembly observed in the simultaneous loss of AKIR-1 and IMA-2 are not due to a reduction in LINC movement.

Loss of both AKIR-1 and IMA-2 results in defects in nuclear import, and chromatin localization of the pairing center protein HIM-8

Mutants that lack all pairing center proteins also show PC formation (Harper *et al.* 2011; Labella *et al.* 2011). Thus, we investigated if the loss of both AKIR-1 and IMA-2 affects the recruitment of HIM-8, the X-chromosome-specific pairing center protein. HIM-8 forms one focus on each X-chromosome, which is observed as two foci when the X-chromosomes are not paired (Phillips *et al.* 2005). When the X-chromosomes pair, these foci are placed in close proximity, which prevents their resolution to two foci, and are therefore counted as one focus per nucleus. We observed no difference in localization patterns of HIM-8 in either *akir-1(gk528)* or *ima-2(ok256)* single mutants compared to wild-type: HIM-8 formed around two foci/nucleus in the

provided on the right of the panel (for more detailed description see Figure 2. A cartoon representing division by zones is indicated on the bottom. (C) Quantification of cytoplasmic HTP-3 PCs throughout the germline of the double mutant *akir-1 ;ima-2*. For *n* values see Table S1. Avg, average; EP, early pachytene; MP, midpachytene; PC, polycomplex; PMT, premeiotic tip; SC, synaptonemal complex; TZ, transition zone.
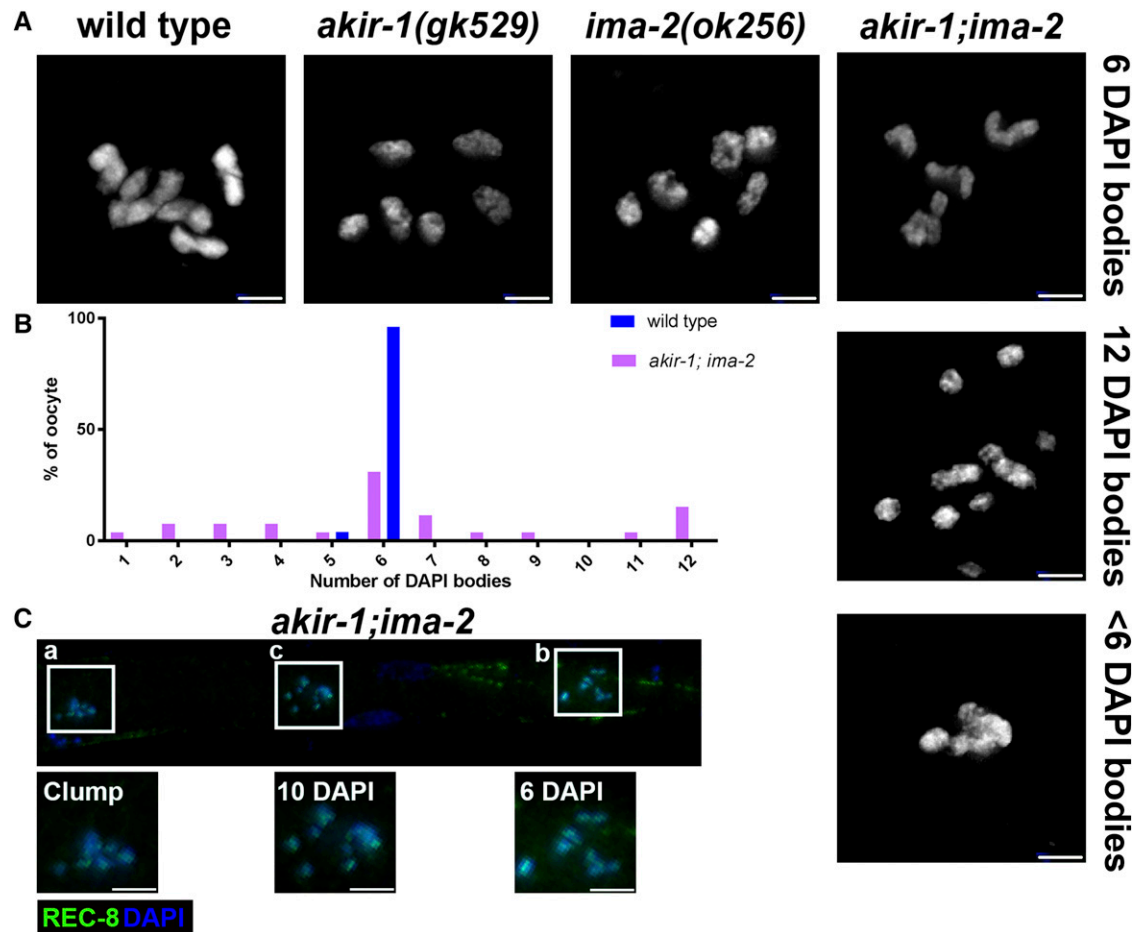
Figure 5 Loss of AKIR-1 and IMA-2 results in defects in crossover formation. (A) DAPI staining of the final diakinesis oocyte prior to fertilization showing condensed chromosomes. The double mutant *akir-1 ;ima-2* displays a wide range of normal number of DAPI bodies in diakinesis-1 oocytes; the image shows representing images of the 6, 12, and < 6 DAPI bodies categories. Bar, 2 μm. (B) Distribution of DAPI body numbers in wild-type and *akir-1 ;ima-2* double mutants; *n* wild-type = 25, *akir-1 ;ima-2* = 26. (C) Example of all three diakinesis phenotypes present in a single germline stained with DAPI (blue) and REC-8 (green). Bar, 3 μm. For *n* values see Table S1.

PMT and 1 focus in the TZ onward (Figure 6, A and B). However, in the double mutant *akir-1(gk528);ima-2 (ok256)*, we found that HIM-8 forms multiple foci around chromosomes/DAPI in the PMT, with the effect becoming more evident after the nuclei enter meiosis (Figure 6, A and B and Figure S6). ZYG-12 can be used as a marker for the nuclear envelope; even in nuclei in which it is found enriched in patches at the nuclear envelope, it marks the whole nuclear envelope with a weaker signal (Figure S4). Analysis of the positions of these aggregates in relation to ZYG-12 indicated that most of these aggregates were associated with the nuclear envelope (Figure S6B), with a population of HIM-8 aggregates that did not come into contact with ZYG-12 (Figure S6, A and C). These foci that did not associate with ZYG-12 were present inside (Figure S6C) and outside the ZYG-12 marker (Figure S6A), and were interpreted as localizing inside and outside of the nucleus, respectively. We also found large cytoplasmic HIM-8 foci aggregates throughout the germline localizing between nuclei (Figure 6C). These aggregates are reminiscent of HTP-3, SYP-1, and

SYP-2 localization in *akir-1(gk528);ima-2(ok256)* double mutants (Figure 2C and Figure 3C). This indicates that the aberrant localization of HIM-8 is not only due to transport defects, but also due to the inability to localize properly to the X-chromosomal pairing center following nuclear import.

Loss of both AKIR-1 and IMA-2 results in the loss of efficient import and aberrant loading of COH-3/4 and REC-8

We have shown that *akir-1(gk528);ima-2(ok256)* double mutants have defects in SC central region and lateral element formation, accompanied by a mislocalization of the pairing center protein HIM-8. In *sun-1(RNAi)* or mutants of *zyg-12*, the ability of chromosomes to pair is lost, but HIM-8 localization remains restricted to the X-pairing center [two foci per nucleus (Sato *et al.* 2009; Woglar *et al.* 2013)]. This phenotype is unlike what we observed for HIM-8 in *akir-1(gk528);-ima-2(ok256)* double mutants. This suggests that loss of HIM-8 attachment to the nuclear envelope does not perturb its ability to localize specifically to two chromosomal sites
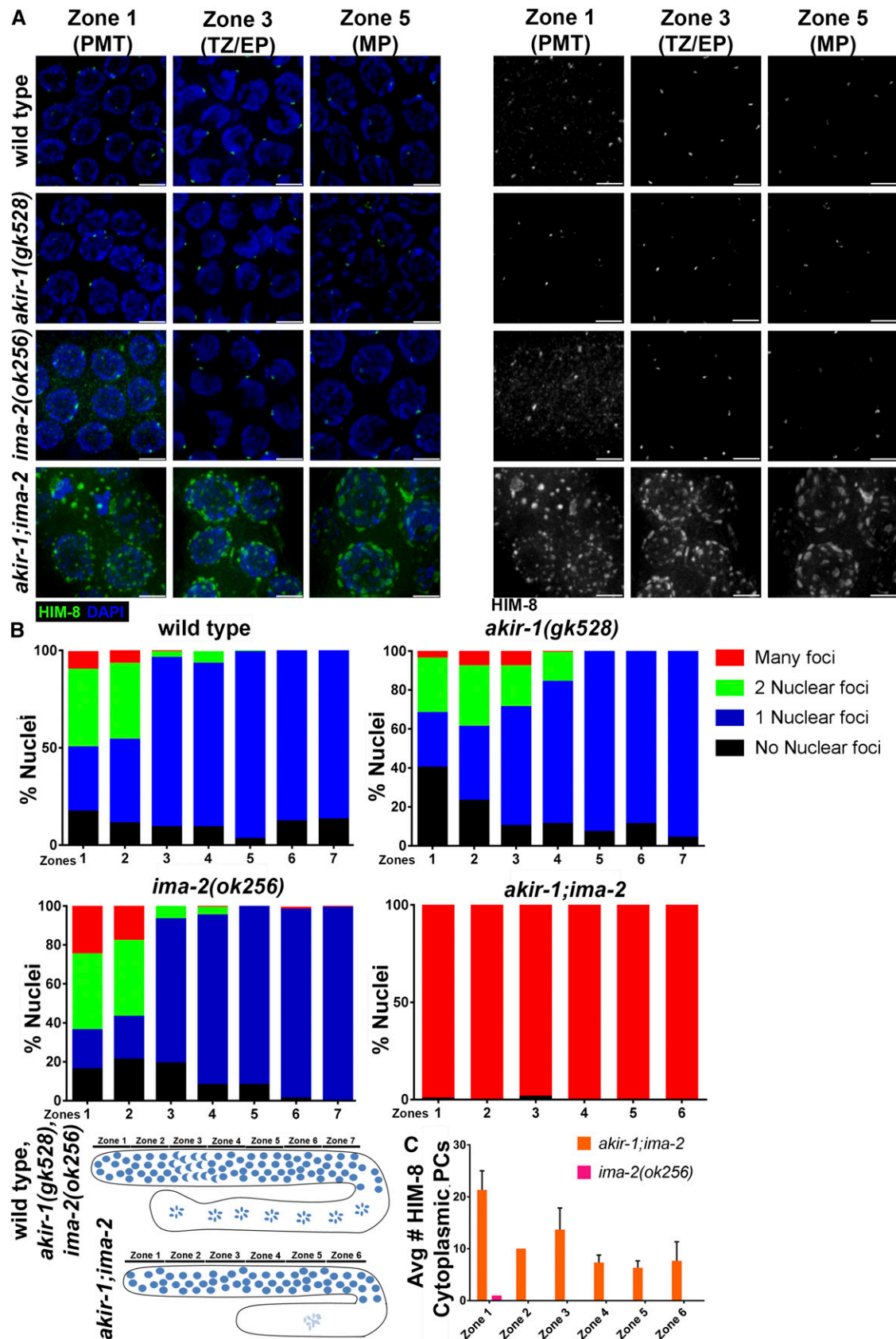
Figure 6 Loss of AKIR-1 and IMA-2 results in loss of efficient nuclear import and localization of HIM-8. (A) Immunolocalization of the X-chromosome pairing center protein HIM-8 for the genotypes indicated. Antibody only channel is presented on the right, *akir-1 (gk528);ima-2(ok256)* shows an

(one at each X-chromosome pairing center) in LINC mutants. We hypothesized that the defect in HIM-8 localization stems from its inability to be recruited to chromosomes in *akir-1-(gk528);ima-2(ok256)* double mutants.

The establishment of sister chromatid cohesion by cohesins is required for SC assembly [both lateral element and central region (Severson 2009; Severson and Meyer 2014), and Figure S7]. Triple mutants of the three SCC-1 like cohesin subunits (REC-8, COH-3, and COH-4) lack all meiotic sister chromatid cohesion complexes (Severson 2009; Severson and Meyer 2014). Interestingly, loss of all meiotic sister chromatid cohesion exhibits a remarkably similar phenotype to that found in *akir-1(gk528);ima-2(ok256)* double mutants. As with *akir-1(gk528);ima-2(ok256)* double mutants, *rec-8;coh-3/4* triple mutants showed similar HIM-8 mislocalization and formed multiple foci surrounding the germline nuclei (Figure S7A).

Next, we examined if the defects in SC assembly stem from defects in the recruitment of the sister chromatid cohesion complex to the germline chromosomes. In wild-type germlines, REC-8 and COH-3/4 assemble in the TZ and localize along the entire length of homologs in middle–late pachytene (Figure 7, A and B and Figure 8, A and B). REC-8, but not COH-3/4, shows nuclear localization in mitotic nuclei prior to meiotic entry (*i.e.*, it is not associated with the chromosomal axis). Similar localization patterns were found in *akir-1(gk528)* and *ima-2(ok256)* mutants (Figure 7, A and B and Figure 8, A and B). However, in *akir-1(gk528);ima-2(ok256)* mutants, we observed aberrant REC-8 and COH-3/4 loading in the germline (Figure 7, A and B and Figure 8, A and B). In the PMT, COH-3/4 localized inside the nuclei, similar to localization of REC-8 at this stage. As nuclei progressed into meiosis, REC-8 and COH-3/4 partially assembled and formed large aggregates in pachytene nuclei, as well as in the cytoplasm (Figure 7B and Figure 8B). The percent of nuclei with REC-8 aggregates was higher than that of COH-3/4 aggregates (Figure 7, A–C and Figure 8, A–C). Staining with SMC-3 in *akir-1(gk528);ima-2(ok256)* double mutants showed similar localization to that of COH-3/4 (Figure S8), consistent with it being part of both REC-8 and COH-3/4 cohesin complexes.

The defects in REC-8 localization were reminiscent of the defects in SC protein localization leading to the formation of PCs. Therefore, we examined the colocalization between the SC and cohesion proteins via double immunostaining for both SYP-1 and REC-8. We found that both proteins colocalized in the meiotic nuclei of all genotypes (Figure S9). Taken together, these data suggest that efficient import and loading of meiotic cohesins and SC proteins requires the presence of both AKIR-1 and IMA-2. These defects in cohesin import and

assembly are the likely cause of the mislocalization of SC and pairing center proteins in these mutants.

Discussion

Here, we identify a redundant role for AKIR-1 and IMA-2 in meiosis, which includes the import and loading of the cohesion complex on meiotic chromosomes. These defects lead to the improper localization and assembly of both lateral element and central region SC proteins, which include axis and central region proteins. Problems in SC assembly likely contributed to the aberrant accumulation of recombination intermediates and the failure to form crossovers in at least one-half of all oocytes. Our studies suggest a novel role for worm Akirin in the import and deposition of proteins essential for proper chromosome structure, and a novel role for IMA-2 in the assembly of the sister chromatid cohesion complex outside of its role in transport.

AKIR-1 and IMA-2 collaborate to ensure proper loading of the meiotic cohesin complex

In the double mutant *akir-1(gk528);ima-2(ok256)*, PCs formed for all SC and sister chromatid cohesin proteins examined (HTP-3, SYP-1, SYP-2, REC-8, COH-3/4, and SMC-3). Co-immunostaining analysis revealed that SYP-2 and HTP-3 colocalize, as does SYP-1 and REC-8. Although we did not test all pairwise comparisons, it is reasonable to propose that all SC and sister chromatid cohesion proteins compose a single PC, and not separate structures in the *akir-1(gk528);ima-2(ok256)* double mutants. The colocalization of SC proteins in a single PC structure is reminiscent of what was found for mutants of all three meiotic cohesin complexes (Severson 2009), except that in *akir-1(gk528);ima-2(ok256)* double mutants the REC-8 and COH-3/4 cohesin complexes are not completely lost. Thus, in the *akir-1(gk528);ima-2(ok256)* double mutant, cohesins can be partially loaded leading to SC assembly in some nuclei. Many studies have shown that SC central region protein loading to chromosomes is dependent on axis and cohesin complex proteins but not vice versa [for example, Smolikov *et al.* (2007) and Severson *et al.* (2009)]. Thus, it is likely that the primary defect of *akir-1(gk528);ima-2(ok256)* double mutants is in recruiting the meiotic axis. HTP-3 is required for REC-8 localization, but not for that of COH-3/4, while REC-8 and COH-3/4 are both required for HTP-3 loading (Severson 2009). Since both REC-8 and COH-3/4 are mislocalized in *akir-1(gk528);ima-2(ok256)* mutants, it is likely that the primary defect in these mutants is in loading cohesins and not lateral element proteins. All three meiotic cohesion

---

aberrant HIM-8 localization to the X-chromosome. Bar, 3 μm. (B) Quantification of the average number of HIM-8 foci per nucleus in the germline from the PMT through late pachytene for all genotypes. The legend provided on the right reflects the number of HIM-8 foci per nucleus. The "Many foci" category includes foci that were too numerous to count, as seen in (A) for the double mutants. A cartoon representing division by zones is indicated on the bottom. (C) Quantification of cytoplasmic HIM-8 aggregates throughout the germline of the double mutant *akir-1 ;ima-2*. For *n* values see Table S1. Avg, average; EP, early pachytene; MP, midpachytene; PMT, premeiotic tip; TZ, transition zone.
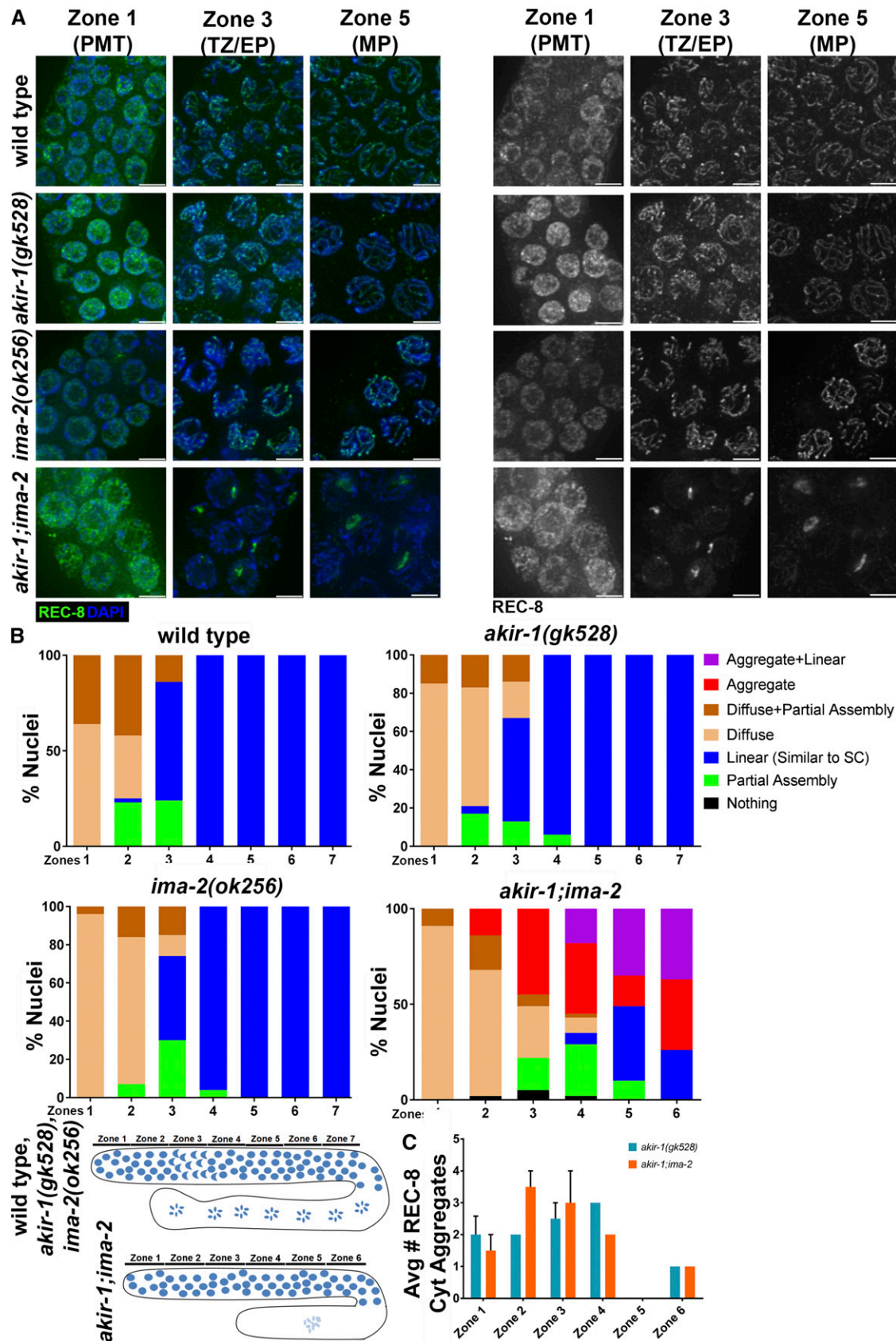
Figure 7 Loss of AKIR-1 and IMA-2 results in the loss of efficient import and aberrant loading of REC-8. (A) Immunolocalization of the cohesin REC-8 for the genotypes indicated. Antibody only channel is presented on the right. Bar, 3 μm. (B) REC-8 is mislocalized in *akir-1 (gk528);ima- 2(ok256)* double

complexes are compromised in *akir-1(gk528);ima-2(ok256)* double mutants.

The most parsimonious model that explains our finding is that the combined action of AKIR-1 and IMA-2 regulates a common subunit of the three complexes in a way that leads to proper assembly of sister chromatid cohesion on meiotic chromosomes (Figure S10). This subunit may be SCC-3, SMC-1, or SMC-3. In agreement, a recent study identified by mass spectrometry a protein–protein interaction between AKIR-1 and SMC-1, and AKIR-1 and SMC-3, in *C. elegans* (Polanowska *et al.* 2018). These were only two of the 53 interactions identified in this study and a biological function for these interactions was not identified. Our study provides a biological function to the AKIR-1-SMC-1 and AKIR-1-SMC-3 interactions. Whether AKIR-1 regulates cohesin loading in somatic nuclei remains to be determined. Our studies also suggest a role for α-importin not only in nuclear import, but also in the deposition of sister chromatid cohesion. This function is indeed novel, but not completely unexpected, as α-importins were shown to be involved in transcriptional regulation, directly and independently of their role in nuclear import (Miyamoto *et al.* 2016)

Despite their important role in forming proper sister chromatid cohesin complexes, AKIR-1 and IMA-2 are not absolutely required for this process. By late pachytene in *akir-1(gk528);ima-2(ok256)* double mutants, many nuclei contain stretches of REC-8 and COH-3/4 (even in the presence of PCs), and 24 DAPI bodies are not observed [as found in *rec-8;coh-3/4* sister chromatid cohesion complex triple mutants (Severson 2009)]. Thus, although all three meiotic cohesin complexes show improper localization in *akir-1(gk528);ima-2(ok256)* double mutants, they are only partially affected. This would explain the phenotype of 12 DAPI bodies observed in diakinesis nuclei of *akir-1(gk528);ima-2(ok256)* double mutants. This is similar to that found in diakinesis in null mutants of a subset of genes encoding for cohesin [12 DAPI bodies in *rec-8* single mutants or *coh-3/4* double mutants (Severson 2009)].

Defects in recombination in the presence of a PC

The *akir-1(gk528);ima-2(ok256)* double mutants provide a unique opportunity to observe repair of meiotic DSB in the presence of PCs composed of cohesin, and lateral and central element proteins. Mutants that form a PC that were described prior to this study either specifically affect central region formation [*e.g.*, *csn-5* or *fkb-6* (Brockway *et al.* 2014; Alleva and Smolikove 2017)], or completely lack cohesin or lateral element components [*e.g.*, *htp-3* (Goodyer *et al.* 2008)]. The formation of the SC is crucial for both DSB formation and repair. When lateral elements do not form, recombination intermediates (RAD-51 foci) are absent [*e.g.*, (Goodyer *et al.* 2008)]. Conversely, when central region proteins do not load, recombination intermediates accumulate [*e.g.*, (Colaiácovo *et al.* 2003)]. *csn-5* mutants (specific to the central region) and *akir-1(gk528);ima-2(ok256)* double mutants exhibit a similar phenotype, even regarding penetrance (percentage of nuclei with a SYP-1 PC). However, RAD-51 foci accumulate to a lesser extent in *akir-1(gk528);ima-2(ok256)* double mutants. Since both lateral and central element assembly is compromised in the *akir-1(gk528);ima-2(ok256)* double mutants, we propose that the phenotype observed is a combination of two effects: fewer DSBs are being made due to compromised lateral element assembly and the DSBs formed are not promptly repaired due to defects in the formation of the central region. We did not observe defects in the localization of RAD-51 to the nucleus (*i.e.*, no RAD-51 aggregates or cytoplasmic foci), therefore we propose that the accumulation of RAD-51 foci in *akir-1(gk528);ima-2(ok256)* double mutants stems from defects in SC assembly, and not from a direct role of IMA-2 or AKIR-1 in RAD-51 localization. Interestingly, both *ima-2* and *akir-1* single mutants show a reduction in RAD-51 intermediates compared to wild-type. This suggests that cohesion (and therefore HTP-3 loading) is slightly compromised by the absence of these proteins, but not to the extent visible by the microscopic analysis that we performed or in a way that interferes with SC assembly.

Downstream of the formation of recombination intermediates is their resolution and the formation of crossovers. Sister chromatid cohesion and SC assembly are required for the formation of crossovers, but AKIR-1 and IMA-2 are not absolutely required for cohesin loading. Despite the defects in loading the cohesin complex at the entry to meiotic prophase (and consequently the SC), by late pachytene more than one-half of the nuclei contain stretches of linear SC that often can be found in the same nucleus with a PC. It is possible that partial SC assembly can support the formation of crossovers, as 30% of diakinesis-1 oocytes contain six bivalents. The remaining oocytes show varying degrees of chromosomal defects and ~50% of the oocytes lack any bivalents. This indicates that AKIR-1 and IMA-2 are required for crossover formation, likely through their effect on the SC.

The cohesin complex is required for proper association of pairing center proteins to pairing centers

In the double mutant *akir-1(gk528);ima-2(ok256)*, the pairing center protein HIM-8 is present in nuclei throughout the germline, similar to wild-type, except that it is localized to multiple sites instead of exclusively to the X-chromosome pairing centers. The presence of nuclear HIM-8 foci in these mutants indicates that the defect in HIM-8 localization is not primarily a nuclear import defect. Analysis of the triple

---

mutants. Key is provided to the left of the panel. A cartoon representing division by zones is indicated on the bottom. (C) Quantification of cytoplasmic REC-8 aggregates throughout the germline of the double mutant *akir-1 ;ima-2*. For *n* values see Table S1. Avg, average; EP, early pachytene; MP, midpachytene; PMT, premeiotic tip; SC, synaptonemal complex; TZ, transition zone.
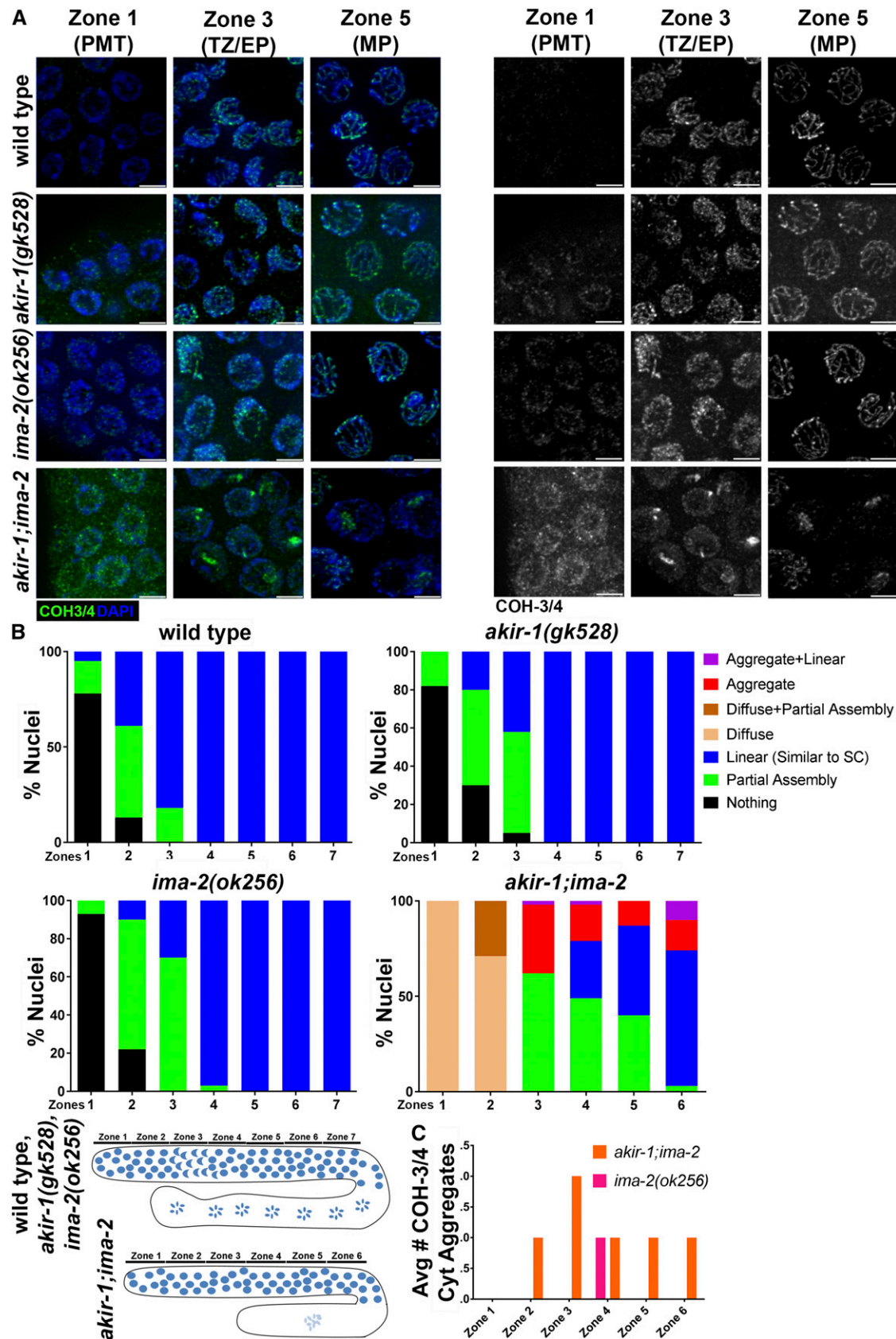
Figure 8 Loss of AKIR-1 and IMA-2 causes COH-3/4 aggregate formation. (A) Immunolocalization of the cohesins COH-3/4 for the genotypes indicated. Antibody only channel is presented on the right. Bar, 3 μm. (B) COH-3/4 are mis localized in *akir- l(gk528);ima-2(ok256)* double mutants. Key is provided

meiotic cohesin knockout *rec-8*;*coh-3*;*coh-4* mutants found the same nuclear envelope localization of HIM-8 as in *akir-1(gk528)*;*ima-2(ok256)* double mutants. This suggests that the presence of cohesins is required for HIM-8 localization specifically to pairing centers. As REC-8 is the only meiotic cohesin to localize to sister chromatids during the last mitotic division prior to meiotic entry, this indicates that the association of REC-8 with chromatin allows HIM-8 to bind a single chromosomal site. Surprisingly, both REC-8 and HTP-3 are present in the mitotic nuclei in *akir-1(gk528)*;*ima-2(ok256)* mutants, but HIM-8 does not form one to two foci but multiple foci at the nuclear envelope, as found in cohesion null mutants. This indicates that in *akir-1(gk528)*;*ima-2(ok256)* mutants, REC-8 likely does not associate with chromosomes in a way that promotes HIM-8 loading. The presence of a zinc finger domain in HIM-8 suggests that HIM-8 binds DNA directly (Phillips *et al.* 2005). Proper cohesin loading may affect chromatin organization, promoting HIM-8 binding to pairing centers and/or restricting HIM-8 from binding to other chromosomal sites.

An alternative possibility is that HIM-8 mislocalization is unrelated to SC/cohesin assembly defects. For example, PLK-1 was shown to be an importin cargo during embryonic development (Martino *et al.* 2017) and PLK-1 was also suggested to play a redundant role with PLK-2 at pairing centers (Harper *et al.* 2011; Labella *et al.* 2011). However, PLK-1/2 association with pairing centers is dependent on pairing center proteins and not vice versa (Harper *et al.* 2011; Labella *et al.* 2011). Due to the striking similarity in the HIM-8 localization pattern between *rec-8*;*coh-3*;*coh-4* mutants and *akir-1(gk528)*;*ima-2(ok256)* mutants, we favor a model by which HIM-8 localization is perturbed by the lack of cohesin binding, as suggested above.

How do AKIR-1 and IMA-2 regulate meiotic cohesion?

The absence of early meiotic defects in *ima-2* or *akir-1* single mutants, and the presence of these defects in the double mutants, is consistent with the hypothesis that these two proteins contribute to the same molecular pathway. AKIR-1 localization to germline nuclei partially requires IMA-2, which may indicate that AKIR-1's nuclear transport is dependent on multiple importins, IMA-2 being one of them. The fact that AKIR-1 is not completely dependent on IMA-2 for its nuclear localization is consistent with a model suggesting redundant roles for the two proteins. The PMT is where cohesin is loaded and becomes cohesive (Severson and Meyer 2014). *akir-1(gk528)*;*ima-2(ok256)* mutants show cytoplasmic aggregates of all proteins examined (SYP-1, SYP-2, HTP-3, HIM-8, REC-8, COH-3/4, and SMC-3), and most of these proteins are found in the nucleus where they fail to assemble properly on chromosomes. These findings suggest that AKIR-1

and IMA-2 play redundant roles in nuclear import and in loading of cohesin proteins. Each one of the proteins is not essential by itself for the pathway, but together they are vital for the accumulation of chromosomally associated cohesin complexes in meiotic nuclei.

The physical interaction observed between AKIR-1 and SMC-1, and AKIR-1 and SMC-3, in *C. elegans* supports a direct role for AKIR-1 in the pathway leading to cohesin loading (Polanowska *et al.* 2018). Unlike what is found for AKIR-1, IMA-2 was not shown to interact with cohesins, thus we do not know if it acts directly on cohesion or on another protein that affects cohesin loading. α-importins do have a nuclear role beside transport (Miyamoto *et al.* 2016), opening the door for a proposed function for IMA-2 in loading cohesins following their import.

The formation of sister chromatid cohesion is divided into several steps: cohesin loading, establishment, and maintenance (Litwin and Wysocki 2018). These steps are molecularly distinct and occur in sequential order. While AKIR-1 and IMA-2 may participate in either one of these steps, we favor the model that they are involved in the first step-cohesin loading. This is supported by our observation that the mislocalization of cohesins in *akir-1(gk528)*;*ima-2(ok256)* mutants is found early on, at the time of cohesin loading. Moreover, COH-3/4 and REC-8 become cohesive by difference mechanisms (Severson and Meyer 2014), while *akir-1* mutants affect both cohesion complexes. The physical interaction studies suggest that AKIR-1 is likely involved with the components common to both complexes, which is consistent with a role in loading *vs.* establishment of cohesin (Polanowska *et al.* 2018).

IMA-2 is known to be involved in nuclear import. Placing AKIR-1 into a model that requires a nuclear import function is more challenging, since AKIR-1 is a nuclear protein involved in the regulation of transcription with no known function in nuclear transport or any known function outside the nucleus (Goto *et al.* 2008; Komiya *et al.* 2008; Nowak *et al.* 2012; Bonnay *et al.* 2014). It is possible that AKIR-1 binds to cohesins while they are transported to the nucleus in a way that is required for their efficient transport.

Loading and unloading SC proteins

AKIR-1 is required for the proper disassembly of the SC; *akir-1* mutants fail to properly disassemble the central region of the SC, leading to PC formation on bivalents of diakinesis oocytes. Unlike SC assembly defects, which are observed only when AKIR-1 loss is combined with the perturbation of IMA-2-mediated nuclear import, the effect of SC disassembly is observed in the single mutants. Moreover, SC assembly defects (*ima-2*;*akir-1* double mutants) affect global chromosome structure (cohesion and all components of the SC),

---

on the right of the panel. A cartoon representing division by zones is indicated on the bottom. (C) Quantification of cytoplasmic COH-3/4 aggregates throughout the germline of the double mutant *akir-1* ;*ima-2*. For *n* values see Table S1. Avg, average; EP, early pachytene; MP, midpachytene; PMT, premeiotic tip; SC, synaptonemal complex; TZ, transition zone.

while SC disassembly (*akir-1* mutants) affects only the central region of the SC. In *ima-2* mutants, AKIR-1 nuclear levels are reduced yet *ima-2* mutants do not show any PC formation upon SC disassembly, as found in *akir-1* mutants. This suggests that the reduced nuclear levels of AKIR-1 in late prophase are sufficient to support normal SC disassembly.

We propose that AKIR-1 is required for SC assembly and disassembly through its regulation of cohesin loading. In *akir-1* single mutants, the effect on the proper deposition of cohesins may be mild, just enough to impede proper disassembly of the SC and to a lesser extent DSB formation (due to its effect on axis formation). Based on the redundancy between *akir-1* and *ima-2*, we suggest that in the absence of AKIR-1, IMA-2 acts in the pathway leading to cohesin loading (Figure S10). However, IMA-2 in the absence of AKIR-1 may load cohesins in a way that is permissive to SC assembly but not SC disassembly. We previously interpreted the phenotype of *akir-1* mutants as rerecruitment of SYPs that have just disassembled back to the chromosome [as opposed to their immediate degradation in wild-type worms (Clemons *et al.* 2013)]. It is possible that the ability to rerecruit SYPs to chromosomes, once SC disassembly is initiated, is affected by the organization of the sister chromatid cohesion complex. The organization of sister chromatid cohesion complexes on the chromosomes may create a structure that is permissive (*akir-1* mutants) or inhibitory (*ima-2* mutants, wild-type) to rerecruitment of SYPs (PC in disassembly). According to this model, AKIR-1 and IMA-2 represent two distinct parts of a pathway that loads cohesins in distinct ways, and/or chromosomal locations, together cooperating in building a functional meiotic axis.

Acknowledgments

Literature Cited

Adam, S. A., 2009   The nuclear transport machinery in Caenorhabditis elegans: a central role in morphogenesis. Semin. Cell Dev. Biol. 20: 576–581. https://doi.org/10.1016/j.semcdb.2009.03.013

Alleva, B., and S. Smolikove, 2017   Moving and stopping: regulation of chromosome movement to promote meiotic chromosome pairing and synapsis. Nucleus 8: 613–624. https://doi.org/10.1080/19491034.2017.1358329

Alleva, B., N. Balukoff, A. Peiper, and S. Smolikove, 2017   Regulating chromosomal movement by the cochaperone FKB-6 ensures timely pairing and synapsis. J. Cell Biol. 216: 393–408. https://doi.org/10.1083/jcb.201606126

Bonnay, F., X. H. Nguyen, E. Cohen-Berros, L. Troxler, E. Batsche *et al.*, 2014   Akirin specifies NF-κB selectivity of Drosophila innate immune response via chromatin remodeling. EMBO J. 33: 2349–2362. https://doi.org/10.15252/embj.201488456

Bosch, P. J., L. C. Fuller, C. M. Sleeth, and J. A. Weiner, 2016   Akirin2 is essential for the formation of the cerebral cortex. Neural Dev. 11: 21. https://doi.org/10.1186/s13064-016-0076-8

Brockway, H., N. Balukoff, M. Dean, B. Alleva, and S. Smolikove, 2014   The CSN/COP9 signalosome regulates synaptonemal complex assembly during meiotic prophase I of Caenorhabditis elegans. PLoS Genet. 10: e1004757. https://doi.org/10.1371/journal.pgen.1004757

Chen, X., Y. Luo, B. Zhou, Z. Huang, G. Jia *et al.*, 2015   Effect of porcine Akirin2 on skeletal myosin heavy chain isoform expression. Int. J. Mol. Sci. 16: 3996–4006. https://doi.org/10.3390/ijms16023996

Clemons, A. M., H. M. Brockway, Y. Yin, B. Kasinathan, Y. S. Butterfield *et al.*, 2013   Akirin is required for diakinesis bivalent structure and synaptonemal complex disassembly at meiotic prophase I. Mol. Biol. Cell 24: 1053–1067. https://doi.org/10.1091/mbc.e12-11-0841

Colaiácovo, M. P., A. J. MacQueen, E. Martinez-Perez, K. McDonald, A. Adamo *et al.*, 2003   Synaptonemal complex assembly in C. elegans is dispensable for loading strand-exchange proteins but critical for proper completion of recombination. Dev. Cell 5: 463–474.

Couteau, F., and M. Zetka, 2005   HTP-1 coordinates synaptonemal complex assembly with homolog alignment during meiosis in C. elegans. Genes Dev. 19: 2744–2756. https://doi.org/10.1101/gad.1348205

de la Fuente, J., C. Almazán, U. Blas-Machado, V. Naranjo, A. J. Mangold *et al.*, 2006   The tick protective antigen, 4D8, is a conserved protein involved in modulation of tick blood ingestion and reproduction. Vaccine 24: 4082–4095. https://doi.org/10.1016/j.vaccine.2006.02.046

Geles, K. G., and S. A. Adam, 2001   Germline and developmental roles of the nuclear transport factor importin alpha3 in C. elegans. Development 128: 1817–1830.

Geles, K. G., J. J. Johnson, S. Jong, and S. Adam, 2002   A role for Caenorhabditis elegans importin IMA-2 in germ line and embryonic mitosis. Mol. Biol. Cell 13: 3138–3147. https://doi.org/10.1091/mbc.e02-02-0069

Goldfarb, D. S., A. H. Corbett, D. A. Mason, M. T. Harreman, and S. A. Adam, 2004   Importin alpha: a multipurpose nuclear-transport receptor. Trends Cell Biol. 14: 505–514. https://doi.org/10.1016/j.tcb.2004.07.016

Goodyer, W., S. Kaitna, F. Couteau, J. D. Ward, S. J. Boulton *et al.*, 2008   HTP-3 links DSB formation with homolog pairing and crossing over during C. elegans meiosis. Dev. Cell 14: 263–274. https://doi.org/10.1016/j.devcel.2007.11.016

Goto, A., K. Matsushita, V. Gesellchen, L. El Chamy, D. Kuttenkeuler *et al.*, 2008   Akirins are highly conserved nuclear proteins required for NF-kappaB-dependent gene expression in drosophila and mice. Nat. Immunol. 9: 97–104 (erratum: Nat Immunol. 9: 216). https://doi.org/10.1038/ni1543

Harper, N. C., R. Rillo, S. Jover-Gil, Z. J. Assaf, N. Bhalla *et al.*, 2011   Pairing centers recruit a Polo-like kinase to orchestrate meiotic chromosome dynamics in C. elegans. Dev. Cell 21: 934–947. https://doi.org/10.1016/j.devcel.2011.09.001

Komiya, Y., N. Kurabe, K. Katagiri, M. Ogawa, A. Sugiyama *et al.*, 2008   A novel binding factor of 14–3-3beta functions as a transcriptional repressor and promotes anchorage-independent growth, tumorigenicity, and metastasis. J. Biol. Chem. 283: 18753–18764. https://doi.org/10.1074/jbc.M802530200

Labella, S., A. Woglar, V. Jantsch, and M. Zetka, 2011 Polo kinases establish links between meiotic chromosomes and cytoskeletal forces essential for homolog pairing. Dev. Cell 21: 948–958. https://doi.org/10.1016/j.devcel.2011.07.011

Litwin, I., and R. Wysocki, 2018 New insights into cohesin loading. Curr. Genet. 64: 53–61. https://doi.org/10.1007/s00294-017-0723-6

Liu, X., Y. Xia, J. Tang, L. Ma, C. Li et al., 2017 Dual roles of Akirin2 protein during Xenopus neural development. J. Biol. Chem. 292: 5676–5684. https://doi.org/10.1074/jbc.M117.777110

MacQueen, A., M. P. Colaiácovo, K. McDonald, and A. M. Villeneuve, 2002 Synapsis-dependent and -independent mechanisms stabilize homolog pairing during meiotic prophase in C. elegans. Genes Dev. 16: 2428–2442. https://doi.org/10.1101/gad.1011602

MacQueen, A. J., C. M. Phillips, N. Bhalla, P. Weiser, A. M. Villeneuve et al., 2005 Chromosome sites play dual roles to establish homologous synapsis during meiosis in C. elegans. Cell 123: 1037–1050. https://doi.org/10.1016/j.cell.2005.09.034

Marshall, A., M. S. Salerno, M. Thomas, T. Davies, C. Berry et al., 2008 Mighty is a novel promyogenic factor in skeletal myogenesis. Exp. Cell Res. 314: 1013–1029. https://doi.org/10.1016/j.yexcr.2008.01.004

Martinez-Perez, E., and A. M. Villeneuve, 2005 HTP-1-dependent constraints coordinate homolog pairing and synapsis and promote chiasma formation during C. elegans meiosis. Genes Dev. 19: 2727–2743. https://doi.org/10.1101/gad.1338505

Martino, L., S. Morchoisne-Bolhy, D. K. Cheerambathur, L. Van Hove, J. Dumont et al., 2017 Channel nucleoporins recruit PLK-1 to nuclear pore complexes to direct nuclear envelope breakdown in C. elegans. Dev. Cell 43: 157–171.e7. https://doi.org/10.1016/j.devcel.2017.09.019

Mehta, G. D., R. Kumar, S. Srivastava, and S. K. Ghosh, 2013 Cohesin: functions beyond sister chromatid cohesion. FEBS Lett. 587: 2299–2312. https://doi.org/10.1016/j.febslet.2013.06.035

Miyamoto, Y., K. Yamada, and Y. Yoneda, 2016 Importin α: a key molecule in nuclear transport and non-transport functions. J. Biochem. 160: 69–75. https://doi.org/10.1093/jb/mvw036

Nowak, S. J., H. Aihara, K. Gonzalez, Y. Nibu, and M. K. Baylies, 2012 Akirin links twist-regulated transcription with the brahma chromatin remodeling complex during embryogenesis. PLoS Genet. 8: e1002547. https://doi.org/10.1371/journal.pgen.1002547

Paix, A., Y. Wang, H. E. Smith, C. Y. Lee, D. Calidas et al., 2014 Scalable and versatile genome editing using linear DNAs with microhomology to Cas9 Sites in Caenorhabditis elegans. Genetics 198: 1347–1356. https://doi.org/10.1534/genetics.114.170423

Paix, A., H. Schmidt, and G. Seydoux, 2016 Cas9-assisted recombineering in C. elegans: genome editing using in vivo assembly of linear DNAs. Nucleic Acids Res. 44: e128. https://doi.org/10.1093/nar/gkw502

Pasierbek, P., M. Jantsch, M. Melcher, A. Schleiffer, D. Schweizer et al., 2001 A Caenorhabditis elegans cohesion protein with functions in meiotic chromosome pairing and disjunction. Genes Dev. 15: 1349–1360. https://doi.org/10.1101/gad.192701

Penkner, A., L. Tang, M. Novatchkova, M. Ladurner, A. Fridkin et al., 2007 The nuclear envelope protein Matefin/SUN-1 is required for homologous pairing in C. elegans meiosis. Dev. Cell 12: 873–885. https://doi.org/10.1016/j.devcel.2007.05.004

Phillips, C. M., and A. F. Dernburg, 2006 A family of zinc-finger proteins is required for chromosome-specific pairing and synapsis during meiosis in C. elegans. Dev. Cell 11: 817–829. https://doi.org/10.1016/j.devcel.2006.09.020

Phillips, C. M., C. Wong, N. Bhalla, P. M. Carlton, P. Weiser et al., 2005 HIM-8 binds to the X chromosome pairing center and mediates chromosome-specific meiotic synapsis. Cell 123: 1051–1063. https://doi.org/10.1016/j.cell.2005.09.035

Polanowska, J., J. X. Chen, J. Soulé, S. Omi, J. Belougne et al., 2018 Evolutionary plasticity in the innate immune function of Akirin. PLoS Genet. 14: e1007494. https://doi.org/10.1371/journal.pgen.1007494

Reichman, R., Z. Shi, R. Malone, and S. Smolikove, 2018 Mitotic and meiotic functions for the SUMOylation pathway in the Caenorhabditis elegans germline. Genetics 208: 1421–1441. https://doi.org/10.1534/genetics.118.300787

Sato, A., B. Isaac, C. M. Phillips, R. Rillo, P. M. Carlton et al., 2009 Cytoskeletal forces span the nuclear envelope to coordinate meiotic chromosome pairing and synapsis. Cell 139: 907–919. https://doi.org/10.1016/j.cell.2009.10.039

Severson, A. F., and B. J. Meyer, 2014 Divergent kleisin subunits of cohesin specify mechanisms to tether and release meiotic chromosomes. Elife 3: e03467. https://doi.org/10.7554/eLife.03467

Severson, A. F., L. Ling, V. van Zuylen, and B. J. Meyer, 2009 The axial element protein HTP-3 promotes cohesin loading and meiotic axis assembly in C. elegans to implement the meiotic program of chromosome segregation. Genes Dev. 23: 1763–1778. https://doi.org/10.1101/gad.1808809

Smolikov, S., A. Eizinger, K. Schild-Prufert, A. Hurlburt, K. McDonald et al., 2007 SYP-3 restricts synaptonemal complex assembly to bridge paired chromosome axes during meiosis in Caenorhabditis elegans. Genetics 176: 2015–2025. https://doi.org/10.1534/genetics.107.072413

Smolikov, S., K. Schild-Prüfert, and M. P. Colaiácovo, 2008 CRA-1 uncovers a double-strand break-dependent pathway promoting the assembly of central region proteins on chromosome axes during C. elegans meiosis. PLoS Genetics 4: e1000088. https://doi.org/10.1371/journal.pgen.1000088

Tartey, S., K. Matsushita, A. Vandenbon, D. Ori, T. Imamura et al., 2014 Akirin2 is critical for inducing inflammatory genes by bridging IκB-ζ and the SWI/SNF complex. EMBO J. 33: 2332–2348. https://doi.org/10.15252/embj.201488447

Tartey, S., K. Matsushita, T. Imamura, A. Wakabayashi, D. Ori et al., 2015 Essential function for the nuclear protein Akirin2 in B cell activation and humoral immune responses. J. Immunol. 195: 519–527. https://doi.org/10.4049/jimmunol.1500373

Woglar, A., A. Daryabeigi, A. Adamo, C. Habacher, T. Machacek et al., 2013 Matefin/SUN-1 phosphorylation is part of a surveillance mechanism to coordinate chromosome synapsis and recombination with meiotic progression and chromosome movement. PLoS Genet. 9: e1003335. https://doi.org/10.1371/journal.pgen.1003335

Zickler, D., and N. Kleckner, 1999 Meiotic chromosomes: integrating structure and function. Annu. Rev. Genet. 33: 603–754. https://doi.org/10.1146/annurev.genet.33.1.603

Communicating editor: J. Engebrecht